NASA TECHNICAL MEMORANDUM

NASA TM X-2192

NASA TM X-2192

UNSTART AND STALL INTERACTIONS BETWEEN A TURBOJET ENGINE AND AN AXISYMMETRIC INLET WITH 60-PERCENT INTERNAL-AREA CONTRACTION

by David A. Choby, Paul L. Burstadt, and James E. Calogeras

Lewis Research Center

Cleveland, Ohio 44135

NATIONAL AERONAUTICS AND SPACE ADMINISTRATION • WASHINGTON, D. C. • MARCH 1971

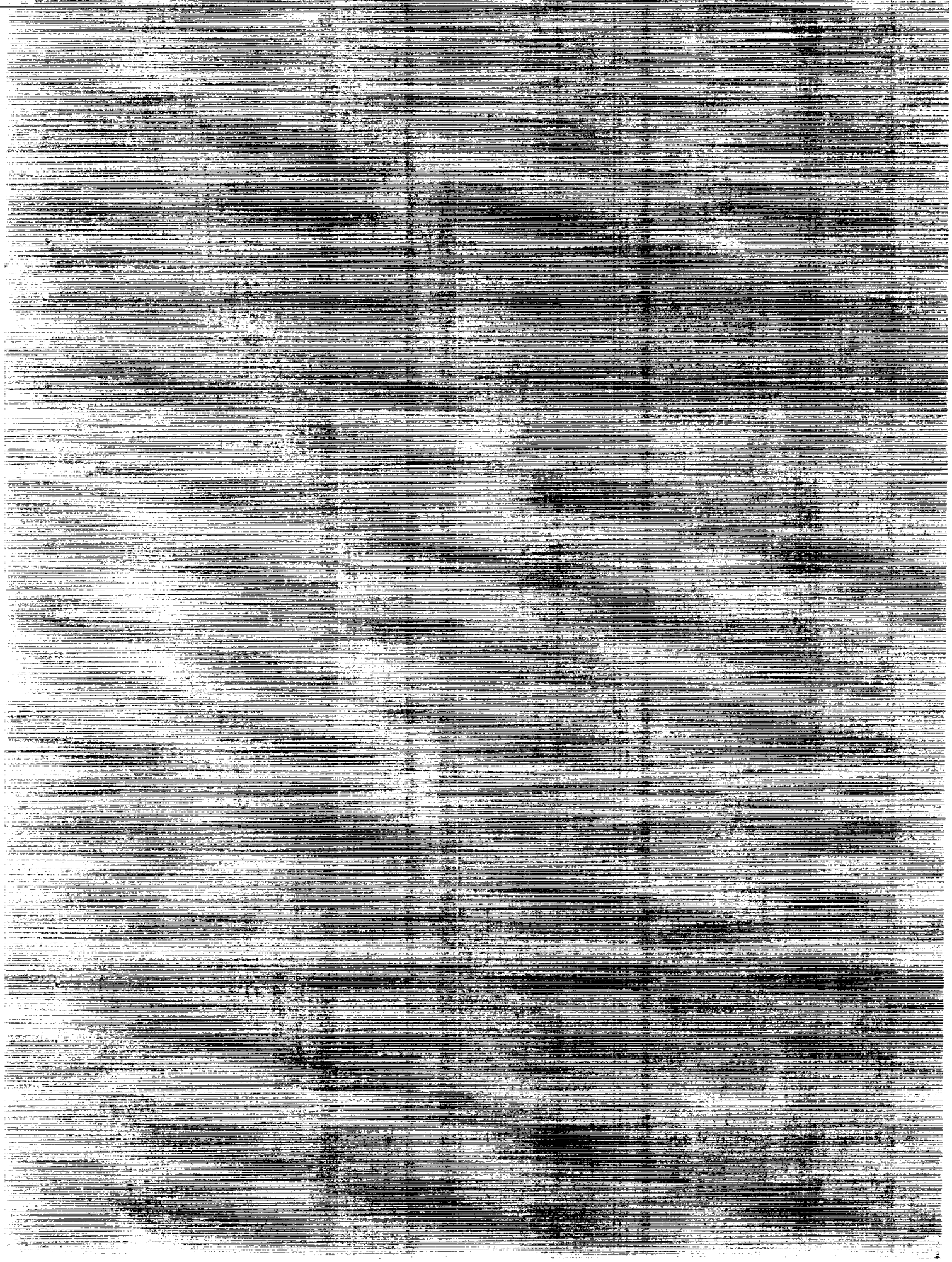

1. Report No.	2. Government Accession No.	3. Recipient's Catalog No.
NASA TM X-2192		

4. Title and Subtitle	5. Report Date
UNSTART AND STALL INTERACTIONS BETWEEN A TURBOJET ENGINE AND AN AXISYMMETRIC INLET WITH 60-PERCENT INTERNAL-AREA CONTRACTION	March 1971
	6. Performing Organization Code
7. Author(s)	8. Performing Organization Report No.
David A. Choby, Paul L. Burstadt, and James E. Calogeras	E-5923
	10. Work Unit No.
9. Performing Organization Name and Address	720-03
Lewis Research Center National Aeronautics and Space Administration Cleveland, Ohio 44135	11. Contract or Grant No.
	13. Type of Report and Period Covered
12. Sponsoring Agency Name and Address	Technical Memorandum
National Aeronautics and Space Administration Washington, D. C. 20546	14. Sponsoring Agency Code

15. Supplementary Notes

16. Abstract

The investigation was conducted in the Lewis 10- by 10-Foot Supersonic Wind Tunnel to determine the effects of inlet unstart on engine operation and the characteristics of stall propagation through the compressor and inlet system. With inlet unstarts at Mach 1.98, the instantaneous compressor pressure ratio which stalled the engine correlated with the steady-state value of the stall compressor pressure ratio. The unstart transient was so large at Mach 2.50 that it caused abrupt compressor stall at all engine operating conditions. Compressor stalls obtained by backpressuring the engine at Mach 2.50 initiated hammer shocks through the inlet which caused surface static pressures to exceed freestream total pressure.

17. Key Words (Suggested by Author(s))	18. Distribution Statement
Propulsion system dynamics Supersonic cruise inlets Dynamics of turbojet Compressor stall Supersonic inlet unstart	Unclassified - unlimited

19. Security Classif. (of this report)	20. Security Classif. (of this page)	21. No. of Pages	22. Price*
Unclassified	Unclassified	37	$3.00

*For sale by the National Technical Information Service, Springfield, Virginia 22151

UNSTART AND STALL INTERACTIONS BETWEEN A TURBOJET ENGINE AND AN AXISYMMETRIC INLET WITH 60-PERCENT INTERNAL-AREA CONTRACTION

by David A. Choby, Paul L. Burstadt, and James E. Calogeras

Lewis Research Center

SUMMARY

An investigation of large-scale transient interactions between a high-performance inlet and a J85-GE-13 turbojet engine has been conducted in the Lewis 10- by 10-Foot Supersonic Wind Tunnel at Mach numbers of 1.98 and 2.50. The axisymmetric mixed-compression inlet had a design Mach number of 2.5 and a 60-percent internal-area contraction.

Transients were imposed on the engine at Mach 1.98 by unstarting the inlet. During the mild unstart transient at Mach 1.98 the instantaneous compressor pressure ratio which stalled the compressor equalled the steady-state value of the stall compressor pressure ratio. The more violent unstart transient at Mach 2.5 caused abrupt compressor stall at all engine operating conditions. Compressor stalls at Mach 2.5 were also obtained by backpressuring the engine (decreasing primary nozzle area). Compressor stalls obtained in this manner were not as abrupt as stalls obtained by unstarting the inlet at Mach 2.5. Stall in the compressor could be observed first as a region of disturbance which would rotate in the direction of rotor rotation at approximately one-half rotor speed. This region would grow circumferentially and would encompass the entire compressor after three to four rotor rotations. The largest hammer shock overpressures in the inlet were caused by compressor stalls induced by backpressuring the engine at Mach 2.5. These overpressures could exceed free-stream total pressure but decreased in amplitude as they approached the inlet geometric throat. The ratio of peak compressor face static pressure during a compressor stall to steady-state compressor exit total pressure before stall was observed to be fairly constant over a wide range of compressor pressure ratios at Mach 2.5.

INTRODUCTION

The proper operation and control of a supersonic aircraft propulsion system requires a knowledge of the steady-state and dynamic interactions between the inlet and the engine. In order to investigate this area and the associated control problems, an experimental program is being conducted in the Lewis 10- by 10-Foot Supersonic Wind Tunnel. For the initial tests, an axisymmetric inlet was selected with a design Mach number of 2.5 and with 60 percent of the supersonic area contraction occurring internally. A complete discussion of the aerodynamic design is presented in reference 1. Experimental investigations have optimized the porous bleed system, examined the effect of bleed system backpressure, determined the response of the terminal shock to external and internal disturbances, developed the inlet overboard bypass control system, studied the steady-state inlet-engine interactions, and investigated the effect of unsteady inlet flow on the stall tolerance of a turbojet engine. The results of these investigations are presented in references 2 to 7, respectively.

Although some of these reports have discussed inlet and engine transient performance, most have been limited to the relatively low amplitude transients that are used in studying control systems. The current report considers the larger transients such as inlet unstart and compressor stall and their effects on the propulsion system. The study investigated the effect of inlet unstarts on system performance at Mach numbers of 1.98 and 2.5. Also the effect of compressor stall on a started inlet was investigated by backpressuring the engine to induce stall. Dynamic instrumentation in the compressor was used to observe propagation of stall through the compressor.

SYMBOLS

A	area, ft^2 (m^2)
IGV	compressor inlet guide vanes
M	Mach number
m/m_0	mass flow ratio
N	engine speed, rpm
N*	design engine speed, 16 500 rpm
$N/N^*\sqrt{\theta}$	corrected engine speed ratio
OGV	compressor outlet guide vanes
P	total pressure, lbf/ft^2 (N/m^2)

ΔP difference between maximum and minimum total pressure, lbf/ft^2 (N/m^2)

p static pressure, lbf/ft^2 (N/m^2)

R_c cowl lip radius, 9.315 in. (23.660 cm)

r local radius, in. (cm)

T total temperature, ^oR (K)

x downstream distance from Mach 2.5 design spike tip position, in. (cm)

Δx centerbody forward extension from Mach 2.5 design position, in. (cm)

β size of stall zone, magnitude of included angle, deg

θ local $T/518.7^o$ R (288.1 K)

φ angular location, deg

Subscripts

0 free stream

1 cowl lip station

2 compressor face station

3 compressor exit station

5 turbine exit station

1-n various locations between cowl lip and compressor face station

2-n exit of n^{th} compressor stage

by overboard bypass

max maximum

Superscripts

$\overline{\ }$ average

APPARATUS AND PROCEDURE

Model Details

The axisymmetric mixed-compression inlet used in this investigation was designed for Mach 2.5 operation. An isometric view of the inlet is shown in figure 1. Figure 2 shows a cross section of the inlet-engine system used in this investigation, and figure 3 presents a more detailed cross section of the inlet.

A translating centerbody was used for starting the inlet and for off-design operation. With the inlet operating at the design Mach number, 40 percent of the supersonic flow area contraction was external and 60 percent was internal. External compression was accomplished with a 12.5° half-angle conical centerbody. Internal compression was obtained from the oblique shock generated by the 0° cowl lip and the two reflected oblique shocks plus isentropic compression between these reflected shocks.

The geometric throat was located at $x/R_c = 3.475$, where the average supersonic Mach number was 1.239. At the geometric throat, the centerbody turned sharply from an angle of about 0° to -5.7°, leading to a 1° equivalent conical expansion throat region four hydraulic radii long. The remainder of the subsonic diffuser was designed as an 8° equivalent conical expansion. The required subsonic diffuser length using this criteria was 3.5 cowl lip radii. However, additional length was required because of overboard bypass exit requirements. The resulting length from cone tip to compressor face was 7.72 cowl lip radii. The aft portion of the subsonic diffuser contained three hollow centerbody support struts which divided the diffuser duct into three compartments back to the engine face. Two of these struts were used to duct centerbody bleed flow overboard.

The inlet configuration (shown in fig. 4) is identical to configuration IND' of reference 1. The vortex generators on the centerbody in the subsonic diffuser were installed to prevent separation of flow from the centerbody in the bypass region when large overboard bypass flows were discharged. Performance bleed, which consisted of porous regions on the centerbody and cowl, was located both in the supersonic diffuser and in the throat region of the inlet. However, for this investigation, bleed was only incorporated in the supersonic portion of the diffuser. The total bleed removed by this system was about 3.5 percent of the capture mass flow. About 3 percent of the capture mass flow was bled through the secondary bypass and was used for engine cooling. The overboard bypass was used to match the inlet and engine airflows. Values of length and volume for various sections of the inlet and engine are presented in table I. Additional information regarding inlet area distributions and volumes is presented in reference 4.

The engine used in this study was the J85-GE-13 turbojet engine. This engine incorporates an eight-stage, axial-flow compressor with a sea-level static average pressure ratio per stage of 1.275, which yields an overall pressure ratio of 7.0. The compressor was driven by a two-stage turbine. The compressor variable geometry consisted of interstage bleed valves (bleed was located in the stators of the third, fourth, and fifth compressor stages) and inlet guide vanes. The bleed valves and guide vanes were linked together and on a standard engine would have been scheduled by the main fuel control as a function of corrected speed. However, the main fuel control was bypassed for this investigation. For the portion of the investigation where compressor stall was initiated by an inlet unstart, the compressor variable geometry was controlled by an analog computer

which followed the same schedule as that of the main fuel control, which started opening the bleed as engine corrected speed decreased below 0.94 of the design speed. When compressor stall was caused by backpressuring the engine, the compressor variable geometry was scheduled manually. The manual schedule called for the bleed valves to be closed to the limit dictated by compressor blade vibration at each corrected speed. For this case, the bleed was closed from 90 to 100 percent of design speed. Also, in order to insure that compressor stall would occur before the maximum allowable turbine temperature was reached, a reduced area first-stage turbine stator was installed. The exhaust nozzle, which was normally scheduled by the afterburner fuel control, was set manually for this investigation.

Model Instrumentation

Steady-state and dynamic pressure instrumentation at the compressor face station is presented in figure 5. Total pressure recovery was measured by the two fixed rakes in the lower right duct segment as viewed looking downstream. The rakes were located 5.86 inches (14.88 cm) upstream of the compressor inlet guide vanes. Each 10 tube rake consisted of six equal-area weighted tubes with additional tubes added at each side of the extreme equal area-weighted tubes in positions corresponding to an 18-tube area-weighted rake. Profiles presented in reference 1 indicate axial symmetry of the flow at 0° angle-of-attack. Therefore it was assumed that measurements made in any one of the three duct segments were representative of the entire flow field. Transient total and static pressures at the compressor face were measured by subminiature strain-gage absolute pressure transducers. The total pressure dynamic probe was located 1.25 inches (3.175 cm) upstream of the compressor inlet guide vanes. The total pressure transducer was mounted tangential to the tube to protect the transducer diaphragm from particle damage. The 0.75-inch (1.905-cm) tube length was necessary to obtain an accurate total pressure but still was short enough to yield a flat response to at least 1000 hertz. The compressor-face static-pressure transducer was flush mounted on the cowl at the same axial distance from the compressor inlet guide vanes as the two steady-state rakes.

The compressor discharge pressure was measured by 16 steady-state total-pressure probes mounted in four rakes as shown in figure 6. One of the total-pressure probes was used to measure both steady-state and transient pressures. This was accomplished by flush mounting a piezoelectric transducer to the inside diameter of the probe 6.0 inches (15.24 cm) downstream of the probe entrance. The probe inside diameter was held constant 15 feet (4.57 m) downstream of the transducer, which was sufficient length to produce a nearly nonresonant line. The line was then connected to the steady-state data-recording system.

One dynamic total-pressure probe, five dynamic static-pressure taps, and five steady-state static pressure taps were located through the inlet as shown in figure 7. The outputs of the strain-gage absolute-pressure transducers incorporated in the cowl-lip static-pressure tap and the throat total pressure probe were used in ratio form to sense inlet unstart. The cowl-lip static and throat total probe transducers were mounted at the ends of 15- and 2-inch (38.1- and 5.08-cm) long lines, respectively. The remaining four transducers were of the piezoelectric type and were flush mounted on the cowl surface.

Steady-state instrumentation in the compressor consisted of two axial rows of static taps. Each row had a static tap at the exit of each stator. The circumferential location of each row is shown in figure 8. Transient interstage static taps were also located at the exit of each stator. The transducers used to measure the interstage transient static pressures were mounted at the end of 2.0-inch (5.08-cm) lines.

The frequency responses of the various pneumatic systems used to measure transient pressures are shown in figure 9. The cowl lip static and throat-exit total pressures were used only to sense inlet unstart by noting a change in the ratio of the two pressures. Therefore, the frequency responses of these two pressure measurement systems are not presented.

Turbine discharge temperature was measured by the eight thermocouples shown in figure 10, which were installed by the engine manufacturer and wired in parallel to give an average reading. The engine speed was measured by a magnetic pickup which sensed the tooth passage of a rotating gear which was attached to the customer power takeoff shaft from the engine gearbox. The positions of the inlet centerbody and overboard bypass doors were determined from potentiometer measurements.

All dynamic data were recorded on FM tape and played back on a light beam oscillograph. The record and playback systems were limited to 1000-hertz information. The combination of the light beam oscillograph and the 1000-hertz filters yielded a flat signal response to 600 hertz.

RESULTS AND DISCUSSION

The results of this investigation will be discussed in three sections: (1) the effect of inlet unstart on engine operation, (2) the propagation of stall through the compressor, and (3) inlet overpressures due to stall.

Presented in figure 11 are the relative magnitudes of the inlet unstarts at Mach 2.50 and Mach 2.02 which were determined in prior isolated inlet tests with a choked plug. These data are representative of the unstart transients imposed on the inlet-engine combination during the present investigation. The data presented is the time average of the unsteady conditions recorded on the steady-state data recording system. When the inlet

was unstarted at Mach 2.5 (fig. 11(a)) the inlet went into an unstable condition. It will be shown later that during this unstable condition the compressor face pressure recovery varied between values of 0.20 and 0.60. The unstart at Mach 2.02 (fig. 11(b)) was a much milder transient. Inlet conditions immediately after unstart at Mach 2.02 were stable. The compressor face total pressure recovery initially dropped to a value of 0.75 as the terminal shock was first expelled but then leveled out at a value of 0.83. This initial drop could not be recorded with the steady-state data system.

Effect of Inlet Unstart on Engine Operation

At Mach 1.98 the inlet was unstarted from the peak total pressure recovery (0.93) condition by slowly closing the overboard bypass doors and leaving them in the unstart position. The inlet unstart at Mach 1.98 was relatively mild as the total pressure recovery only dropped from 0.93 to 0.71 during the unstart transient. The inlet was unstarted with the engine operating at corrected speed ratios of 0.86, 0.90, and 0.935. At a given engine speed, unstarts were obtained for various values of initial exhaust nozzle flow area which were gradually decreased to provide increasing initial compressor pressure ratios until an initial operating condition was found where the unstart would cause a compressor stall. During the stall the turbine temperature usually dropped, indicating a combustor blowout. The locus of these points (fig. 12) defines the limit of the region where the engine would remain operating during a Mach 1.98 unstart transient. Only at a corrected speed ratio of 0.86 was an operating point found where the combustor remained lit through a compressor stall, allowing continued engine operation. All other stalls caused by inlet unstart were followed by combustor blowout and loss of engine power.

The operating points where an unstart produced stall were about midway between the normal operating line and the zero distortion stall line. Thus the mild unstart during normal engine operation at Mach 1.98 would not produce a compressor stall within the speed range investigated.

Time histories of inlet and engine parameters during inlet unstarts at Mach 1.98 are presented in figure 13. These data correspond to the three compressor pressure ratios (fig. 12) at 0.86 corrected speed ratio. The time histories of the higher speed points of the previous figure were similar to the lower speed points and thus are not shown. The unstart can be seen as an increase in the ratio of cowl lip static to throat total pressure at zero time. The unstart triggered a control sequence which, after a preset delay time, automatically chopped the engine throttle, opened the overboard bypass, extended the spike, and opened the exhaust nozzle.

Many of the transducers used in this study were of the piezoelectric type and the dc

output of the subminiature strain gage transducers was not reliable. Therefore steady-state data were obtained on a separate recording system prior to each unstart and were used as initial values for dynamic data. The initial value for the compressor exit pressure was the average of the 16 compressor exit steady-state tubes shown in figure 6. The initial value for the compressor face pressure was the average of the 20 steady-state compressure face tubes shown in figure 5. However, the pressure variation with time is only a single transient pressure measurement. The dc outputs of the transducers were used to obtain the initial value of the ratio of cowl lip static to throat total pressure. The initial values for engine exhaust gas temperature, engine rotor speed, spike position, and overboard bypass area were obtained from the steady-state recording of the same pickups as were recorded dynamically. The initial and final overboard bypass areas are shown; however, the calibration between these two points is not linear. The exhaust gas temperature signal was passed through a 10-hertz filter before being recorded on the oscillograph.

Figure 13(a) shows the time history of the inlet unstart with the compressor operating at an initial pressure ratio of 4.56. Here the delay time (before the geometry is varied after unstart) is a little over a second. At this time the overboard bypass area is seen to increase as the spike extends. Also, engine rotor speed and turbine discharge temperature begin to decrease. It should be noted that until this time turbine discharge temperature and engine speed have remained constant through the transient, implying continuous engine operation. The pressures at the compressor face and discharge are seen to drop immediately after unstart. However, the compressor face pressure shows no hammershock which suggests that the compressor did not stall.

Figure 13(b) presents the time history of the inlet unstart with the compressor operating at a pressure ratio of 4.69. The delay time used was 0.6 second. Engine speed and turbine discharge temperature behaved the same as in figure 13(a). An examination of the compressor face pressure shows the presence of a hammer shock indicating compressor stall. Immediately after the hammer shock the compressor face and discharge total pressures decreased rapidly to very low values and then recovered. This initial transient occurred in just under 0.1 second. The presence of the hammer shock together with the undisturbed turbine discharge temperature and engine speed suggest a compressor stall and recovery with continuous engine operation.

Figure 13(c) shows the unstart time history with the compressor operating at a pressure ratio of 4.87. Again, a time delay of 0.6 second was used. The initial transient shows a hammer shock at the compressor face indicating compressor stall. Engine rotor speed and turbine discharge temperature begin to decrease immediately after unstart indicating a probable combustor blowout. Within 0.1 second after unstart the compressor face pressure has recovered from a very low value. If there were combustor blowout, the compressor discharge pressure would not recover as in the previous case, since the

engine would now be windmilling and the compressor pressure ratio would be lowered. The fact that the compressor discharge pressure partially recovers indicates that the stall has probably cleared. Compressor discharge pressure remains fairly stable for 0.15 second. This further suggests that the stall has cleared. Approximately 0.2 second after the unstart a cyclic pressure disturbance of about 24 hertz is seen at the compressor face and discharge stations. This cyclic disturbance is most likely inlet buzz. The decreasing rotor speed would cause the compressor to demand less airflow which could drive the inlet into unstable operation. This situation is not alleviated until the overboard bypass doors begin to open at 0.6 second after the unstart.

At Mach 1.98, the time from the beginning of the unstart transient to compressor stall was on the order of three rotor rotations. This suggests that it would be possible to correlate the maximum dynamic compressor pressure ratio with the steady-state stall limit of the compressor. Dynamic pressure ratios are presented in figure 14 for the same operating conditions shown in figure 13.

At time zero, the compressor face total pressure recovery was about 0.90 for each condition presented in figure 14. The initial value of compressor exit total pressure ratioed to free-stream total pressure was a function of initial compressor pressure ratio and increasing values are shown in figures 14(a) to 14(c), respectively. For the first 15 milliseconds of the transient the compressor face pressure behaved similarly for all three cases; that is, it dropped from 0.90 to about 0.75. The compressor face pressure began to drop immediately after time zero while there was a 5-millisecond delay until compressor exit total pressure began to drop. This time delay of the transient through the compressor caused the compressor pressure ratio to increase and reach a maximum value at about 7 milliseconds. The increase in compressor pressure ratio for the three parts of figure 14 is about the same. But since the initial values of compressor pressure ratio were different, the maximum values reached during the transient were different.

In part (a), the maximum transient compressor pressure ratio was about 5.0, and the steady-state stall compressor pressure ratio was about 5.2. Thus the steady-state stall limit of the compressor was not reached during the transient. The compressor pressure ratio remained at a maximum for about 8 milliseconds and then returned to the initial value. The compressor face pressure recovery, after reaching a low of about 0.75, increased at 25 milliseconds to about 0.85 and remained stable. The compressor exit pressure decreased during the transient and settled out at a value which would give the same compressor pressure ratio for the new compressor face pressure.

In figure 14(b), the maximum compressor pressure ratio reached a value of 5.2 which was the same as the steady-state stall compressor pressure ratio. At about 17 milliseconds the compressor pressure ratio dropped precipitously from about 5.2 to about 3.0, indicating compressor stall. An overpressure slightly greater than free-stream total pressure is seen at the compressor face as the stall-induced hammer shock

moves upstream through the inlet. At this same time the compressor exit total pressure is seen to decrease sharply. The overpressure is seen at the compressor face for about 10 milliseconds. Following the compressor face overpressure the compressor face pressure recovery dropped to about 0.30. At about 55 milliseconds the compressor face total pressure recovery settles out at a value of 0.85. The compressor pressure ratio reached a low of 2.0 at 26 milliseconds, recovered to a value of 4.0, and again fell sharply at 45 milliseconds to a value of 2.0. It then recovered at 65 milliseconds to nearly the initial operating value. As shown in figure 13(b), it was noted that for this case the compressor stalled and cleared with continuous engine operation.

In figure 14(c), the maximum compressor pressure ratio reached a value of about 5.3 which was greater than the steady-state stall compressor pressure ratio. At about 17 milliseconds, the compressor pressure ratio fell sharply. This was accompanied by a sharp overpressure at the compressor face due to the stall induced hammer shock and a drop in pressure at the compressor exit. At 50 milliseconds, the compressor face pressure recovery stabilized at 0.85. The compressor pressure ratio also stabilized at about this time at a value of 3.0. The uniform pressures after 50 milliseconds suggest that the stall has cleared but the low value of compressor pressure ratio would indicate the engine is now windmilling. Figure 12(c) showed that for this case the compressor stalled and the combustor blew out.

As figure 14 shows, the engine will stall if the maximum value of the dynamic compressor pressure ratio during an inlet unstart exceeds the steady-state stall line. This correlation between the maximum value of compressor pressure ratio and the steady-state stall limit also existed for the higher engine speed data shown in figure 12. It should be noted, however, that the dynamic compressor pressure ratio is a ratio of the output of two transducers and therefore cannot give a true representation of the entire flow field. The initial value was obtained by forming a ratio of the two initial values obtained from steady-state rakes. The two transducers that were used to form the ratio were 40 degrees out of alinement. Because of these limitations, it may be somewhat fortuitous that the correlation is as good as indicated for the Mach 1.98 data.

The effect of unstarting the inlet was also investigated at a Mach number of 2.5. At Mach 2.5 it was impossible to unstart the inlet by closing the bypass doors without going into violent buzz. Thus, any unstart at Mach 2.5 was made with a closed-loop terminal shock control system. The terminal shock control feedback signal was a throat-exit static pressure, and the overboard bypass doors were the manipulated variable. To unstart the inlet while on closed loop control, the throat-exit pressure command signal was instantaneously scheduled to a high value that the inlet could not provide. While attempting to reach this value, the bypass doors moved toward the closed position and the inlet unstarted. At this point the control system sensed the unstart (by the ratio of cowl lip static to throat total pressure) and the throat-exit pressure command was reduced to a

much lower value which caused the doors to open. The unstart signal also initiated centerbody translation (at a fixed rate) in order to effect inlet restart by increasing the throat to capture area ratio. During centerbody translation, the throat-exit pressure command was scheduled as a function of centerbody position. When the control system sensed a restart (via the unstart signal), the centerbody reversed direction and the throat-exit pressure command followed a new schedule as a function of centerbody position. When the centerbody returned to the design position, the throat-exit pressure command was returned to the design value. This control system is reported in detail in reference 5. Two seconds after the initiation of the transient, the engine system was shut down as described previously for the data shown in figure 13.

The transients following a Mach 2.5 unstart are shown in figure 15. Engine speed decreased immediately and the turbine discharge temperature began to decrease in less than 10 milliseconds suggesting compressor stall and combustor blowout. However, only a weak hammer shock is visible at the compressor face. The compressor discharge pressure decreases and does not recover for several tenths of a second which suggests that the stall did not clear immediately. This particular stall is typical of compressor stall induced by a Mach 2.5 unstart and is presented in more detail in figures 16 and 17.

Figure 16 presents the details of the compressor inlet and exit pressure ratios during unstart and stall. The unstart at Mach 2.5 causes the compressor face total pressure recovery to decrease from 0.93 to 0.40 in less than two rotor rotations (about 4 msec per rotation) after unstart. The decrease in compressor discharge pressure occurs about 5 milliseconds after the fast decrease in compressor face pressure. This delay of the transient through the compressor caused the dynamic compressor pressure ratio to rise significantly above the steady-state stall limit. Apparently because of the very high transient pressure ratio, the stall at Mach 2.5 was complete in less than two rotor rotations after unstart compared with four rotor rotations at Mach 1.98.

For all cases of compressor stall a hammer shock was generated to adjust the inlet flow to the near zero flow requirements of the compressor. When the inlet was unstarted at Mach 2.5, the hammer shock generated was observed to be weak. This may be caused by the Mach 2.5 unstart being a large enough transient to nearly stagnate the incoming flow at the compressor. Thus only a weak hammer shock was needed to satisfy the flow requirements of the stalled compressor.

Stall Propagation Within the Compressor

The dynamic instrumentation shown in figure 8 provided time histories of static pressures at the exits of various compressor stages and compressor exit total pressures which are presented in figure 17. Transient measurements of compressor inlet static

pressure, cowl lip static pressure, and throat total pressure were also recorded. When stall occurred, this instrumentation provided information about how the stalled region propagated through the compressor.

Stall initially occurred in a circumferential sector of the compressor and it was sometimes possible to determine the axial origin of the stall zone by observing the resulting transient pressures in the compressor. This was done by assuming that rapid pressure increases occurred upstream of the stalled stages, while rapid pressure decreases occurred downstream of the stalled stages. Even though all the stages in the circumferential sector may not be stalled, the region will be called a stall zone. Results (which will be discussed) showed that the stall zone appeared in the compressor as an axial channel, and rotated in the direction of rotor rotation (counterclockwise looking downstream) at about one-half rotor speed. As it rotated, the zone extended through the compressor and widened in the circumferential direction until it encompassed most or all of the compressor. This propagation of stall by rotation is complete within a few rotor rotations and should not be confused with the classical definition of rotating stall.

Transient pressure measurements are presented in figure 17 for the cases of engine stall initiated by

(a) Inlet unstart at $M_0 = 1.98$

(b) Decreasing primary nozzle exit area at $M_0 = 2.5$

(c) Inlet unstart at $M_0 = 2.5$

Reference to the compressor station locations in figure 8 may be helpful during the following discussion. For example, station 2-n refers to the exit of the n^{th} stage stator. The initial values for the compressor face total pressure, the compressor exit total pressure and the ratio of cowl lip static pressure to throat total pressure were obtained in the same manner as was used in figure 13. The initial value of compressor face static pressure was the average of the 12 steady-state static taps shown in figure 5. The initial value for the compressor static pressures was the average of the two steady-state static pressure taps at each stage.

Figure 13(c) presents a time history of inlet and engine parameters for conditions that correspond to the data shown in figure 17(a) (engine stall initiated by inlet unstart at Mach 1.98). In figure 17(a) the pressures begin to fall gradually at $t = 0$ due to unstart, and the stall zone was first observed as a rise in the static pressure at station 2-7 ($\varphi = 70^{\circ}$). This occurred about 8 milliseconds after the rise of the unstart signal (p_{1-1}/P_{1-2}). The static pressure ratios at stations 2-1 and 2-2, which had the same angular location ($\varphi = 70^{\circ}$) did not show any transient pressure change at this time. This indicates that the stall zone originated in the rear stages and had not yet extended into the forward stages. Because of this, there was no observed pressure change at the compressor face (station 2) as the stall zone rotated to $\varphi = 30$.

The stall zone then rotated counterclockwise (looking downstream) and was observed

about 10 milliseconds after unstart at stations 2-3 to 2-5 ($\varphi = 13^{o}$). It appeared as a sharp rise in the static pressures at these locations. This was followed by a sharp drop in compressor exit total pressure ratio at station 3 ($\varphi = 330^{o}$), about 12 milliseconds after the rise of the unstart signal. Rotation of the stalled region continued, causing a pressure increase at stations 2-1 and 2-2 ($\varphi = 70^{o}$) and a decrease at station 2-7 ($\varphi = 70^{o}$). This occurred approximately 16.5 milliseconds after unstart. There was also a rise in static pressure at station 2 ($\varphi = 30^{o}$) at essentially the same time.

About 18 milliseconds after unstart, the rotating stall zone returned to the circumferential location of station 2-3 to 2-5 ($\varphi = 13^{o}$) and reduced these pressures precipitously. The drop in pressure was opposite of the initially observed pressure change at these stations. Rotation of the stall zone continued, leading to another sharp drop in compressor exit total pressure at station 3 ($\varphi = 330^{o}$) about 20 milliseconds after the rise of the unstart signal. One more revolution of the stall zone was observed, and then all pressures began to fall toward their minimum values at approximately 25 milliseconds after unstart.

When sharp pressure increases were observed at station 2-3 to 2-5 ($\varphi = 13^{o}$) about 10 milliseconds after unstart, the pressures reached a peak and then decreased immediately. This sharp drop was followed by a gradual decrease. However, when the pressure dropped sharply at station 2-5, 18 milliseconds after unstart, it stayed near the lower level for an appreciable amount of time (about 3 msec). This trend is less apparent at stations 2-3 and 2-4. This indicates that the included angle of the stall zone β had increased, at least at station 2-5.

With the limited instrumentation, it was not possible to determine the circumferential location of the stall origin. If there had been dynamic instrumentation at many different angular positions the circumferential location of stall origin could have been detected fairly accurately. This could be done by noting the value of φ for the first instrumentation station that registered the type of pressure fluctuations expected during initiation of stall.

As mentioned previously, the second time the rotating stall zone was observed at stations 2-3 to 2-5 ($\varphi = 13^{o}$), it appeared as a sharp reduction in pressure. However, the first observation showed a pressure increase. This tends to indicate that either the axial origin of the stall zone had moved forward from a location aft of stage 7 to the exit of stage 3 during the first stall revolution or the original zone died out and a new zone was formed. From these observations, the period of the rotating stall was determined to be 8 to 9 milliseconds. This corresponds to the expected value of twice the rotor period. Since the time between the pressure fluctuations of the first and second observations at stations 2-3 to 2-5 corresponded to the frequency of rotating stall, the origin of the original stall zone probably moved forward.

Dynamic pressure responses for a compressor stall at Mach 2.50, initiated by de-

creasing the primary nozzle exit area, are presented in figure 17(b). Note that for this case the measurements of the compressor exit total pressure P_3 and the inlet unstart signal are not shown and that the transient static pressure at station 2-6 was included.

The stalled zone was first observed at the $\varphi = 70^{\circ}$ location as a sharp rise in static pressure at stations 2-1 and 2-2, and as a sharp drop in static pressure at stations 2-6 and 2-7. At the same time, a rapid increase in static pressure was seen at the compressor face (station 2, $\varphi = 30^{\circ}$). It appears that the stall zone was well established and extended through the entire compressor, while covering a circumferential range of at least $30^{\circ} \leq \beta \leq 70^{\circ}$. About 1 millisecond later the stalled region had rotated to the $\varphi = 13^{\circ}$ position, which caused a rapid decrease in static pressure at stations 2-3 to 2-5.

After the leading edge of the stalled zone reached the various interstage locations, the pressures attained their maximum or minimum values and then returned to some point close to their initial level. This process, during which the stall zone passed a certain angular location, required about 7 milliseconds and was completed just before the leading edge of the stall zone returned. The time span of 7 milliseconds necessary for the stalled zone to clear a certain circumferential location indicates that the initial size ($30^{\circ} \leq \beta \leq 70^{\circ}$) combined with the growth rate ($d\beta/dt$) produced a stall zone that had covered most of the compressor face within 8 milliseconds after it was first observed.

About 8 milliseconds after the first observation, the leading edge of the stalled region returned to the $\varphi = 70^{\circ}$ location. The pressure increased sharply at station 2-1 and fell off rapidly at stations 2-6 and 2-7, but there was very little pressure change at station 2-2. This was followed approximately 1 millisecond later by an increase in compressor-face static pressure at station 2 ($\varphi = 30^{\circ}$). Rotation of the stalled zone continued, which caused the pressures at stations 2-3 to 2-5 ($\varphi = 13^{\circ}$) to drop sharply. This last passage of the stall zone leading edge was followed by a large drop in pressure at all stations.

After the large pressure decrease between 10 and 20 milliseconds, a cyclic pressure disturbance with a frequency of approximately 130 hertz was observed at all stations. Because this type of disturbance was also seen when this inlet was run without an engine (see ref. 5), it was considered to be a type of inlet instability rather than an engine phenomenon.

Figure 17(c) presents transient pressure measurements at various compressor locations for the case of engine stall caused by an inlet unstart at Mach 2.50. Corresponding inlet and engine parameters are shown in figure 15. The magnitudes of the initial pressure drops indicate that a very large transient was produced. Since the transient was so large, it appears that engine stall was unavoidable. The stall also became more complete in a shorter period of time than the previously discussed stalls, making it difficult to interpret the dynamic pressure changes.

It is apparent that after the stall became complete and the interstage pressures

reached their minimum levels, a type of inlet instability appeared which was similar to that observed in figure 16(b). The frequency ranged from 100 to 130 hertz in this case.

Inlet Overpressures Due to Engine Stall

When the compressor stalled while the inlet was operating in a started mode at Mach 2.5, large overpressures were always observed through the inlet. These overpressures were the result of a hammer shock which formed in the compressor and propagated upstream. When the compressor stalled, its demand for corrected airflow decreased very rapidly and the hammer shock was generated to adjust the inlet flow conditions to the new compressor requirements.

As mentioned previously, the aft portion of the subsonic diffuser contained three hollow centerbody support struts which divided the duct into three compartments back to the engine face. The unsymmetrical nature of the compressor stall, as exemplified by the rotation of the stalled zone shown in figure 17(b), would indicate that measurements made in one of the three ducts may not be identical to the actual conditions in the other two.

Measurements at one circumferential location showed that static pressures in the inlet reached values greater than free-stream total pressure as the hammer shock passed. Figure 18 shows the time histories of pressures at various inlet axial locations, with the values of peak overpressure labeled. Initial values were obtained from the steady-state taps shown in figure 7. For one of the dynamic probes (station 1-4), an average of two taps were used to obtain the initial steady-state value. Station 2 is closest to the compressor face and shows the first sharp rise. As p_2/P_0 increases from 0.80 to 1.10, the slope dp/dt is about constant. This slope changes as p_2/P_0 rises to a peak value of 1.23. Reference 8 shows a p_2/P_0 pressure rise that has a constant slope between initial and peak values. This was for an engine tested in an altitude cell, without an inlet. Reference 9 presents an analytical model of inlet pressures following a compressor stall. Results show that the pressure just behind the hammer shock increases as it moves upstream into the subsonic diffuser. In view of this simulation, the variations of p_2/P_0 in figure 18 apparently are due to an initial hammer shock pressure rise (to 1.10) followed by a second increase (to 1.23) as the hammer shock moves forward and is partially reflected back from the subsonic diffuser area variation. It should be noted, however, that this simulation was based on the simplifying assumption that a single duct existed rather than a multiple flow passage between the support struts and assumed a uniform corrected airflow cutoff at the compressor face rather than a discrete stall zone.

The peak values of p/P_0 caused by the hammer shock are shown in figure 19 for various inlet-engine conditions. Peak hammer shock overpressure reached its highest

value at station 1-5 and then decreased as the hammer shock (or the combined hammer shock and inlet terminal shock) moved upstream. The decrease in hammer shock strength occurs upstream of the three compartments formed by the centerbody support struts. Since stall was unsymmetrical and initially covered only an angular fraction of the compressor, the hammer shock probably did not occur simultaneously in all three ducts. Thus the decrease in hammer shock strength upstream of the three diffuser compartments could be due to diffusion of the hammer shock. However this does not explain why the hammer shock pressure reached its peak just upstream of the overboard bypass plenum.

Figure 20 shows the ratio of maximum transient overpressure in the inlet to compressor discharge total pressure as a function of compressor pressure ratio. The data presented are for various inlet operating conditions and it can be seen that the ratio remains nearly constant, with values between 0.25 and 0.30. Flight data obtained with the F-111 aircraft are presented in reference 10. In reference 9 a similar correlation held over a wide range of altitude and Mach number. Since the F-111 is powered by the TF-30 turbofan engine, it appears that this type of correlation may be applicable for both turbojet and turbofan engines.

SUMMARY OF RESULTS

An investigation of the transient interactions between a Mach 2.50 axisymmetric, mixed-compression inlet and a J85-GE-13 turbojet engine has been conducted in the Lewis 10- by 10-Foot Supersonic Wind Tunnel. The test was conducted at Mach numbers of 1.98 and 2.50 with the following results:

1. Inlet unstarts at Mach 1.98 were rather mild and would not cause compressor stall if the initial compressor operating point was near the normal operating line. The compressor did stall during a Mach 1.98 inlet unstart when the transient value of compressor pressure ratio exceeded the steady-state value of compressor pressure ratio needed to cause stall. During the unstart stall transient, the pressure ratio remained at or just above the stall line about 10 milliseconds (two to three rotor rotations) before stall occurred.

2. For cases of compressor stall caused by inlet unstarts at Mach 1.98 or caused by decreasing the primary nozzle exit area at Mach 2.50, a stall zone was observed in the compressor as an axial channel extending through the compressor and rotating counterclockwise (looking downstream) at one-half rotor speed. Its size expanded circumferentially as it rotated until it included the entire compressor after about three to four rotor rotations.

3. Compressor stall appeared to be unavoidable when the inlet was unstarted at Mach 2.50. The initial stall zone appeared to encompass nearly the entire compressor,

and stall was complete in less than two rotor rotations after unstart compared with four rotor rotations after unstart at Mach 1.98.

4. Unstarting the inlet at Mach 2.50 always caused compressor stall followed by a decrease in engine rotor speed and engine exhaust gas temperature, indicating combustor blowout.

5. Stalls induced by backpressuring the engine at Mach 2.5 produced hammer shocks such that inlet compressor face static pressure exceeded free-stream total pressure by as much as 40 percent. Following a compressor stall initiated by a Mach 1.98 inlet unstart, compressor face total pressure exceeded free-stream total pressure by 10 percent.

6. Peak hammer shock overpressures through the inlet following compressor stall decreased in value near the inlet throat.

7. Peak transient inlet static pressure ratioed to steady-state compressor discharge total pressure remained nearly constant over a wide range of compressor pressure ratios.

Lewis Research Center,
National Aeronautics and Space Administration,
Cleveland, Ohio, October 13, 1970,
720-03.

REFERENCES

1. Cubbison, Robert W.; Meleason, Edward T.; and Johnson, David F.: Performance Characteristics from Mach 2.58 to 1.98 of an Axisymmetric Mixed-Compression Inlet System with 60-Percent Internal Contraction. NASA TM X-1739, 1969.

2. Cubbison, Robert W.; Meleason, Edward T.; and Johnson, David F.: Effect of Porous Bleed in a High-Performance Axisymmetric, Mixed-Compression Inlet at Mach 2.50. NASA TM X-1692, 1968.

3. Sanders, Bobby W.; and Cubbison, Robert W.: Effect of Bleed-System Back Pressure and Porous Area on the Performance of an Axisymmetric Mixed-Compression Inlet at Mach 2.50. NASA TM X-1710, 1968.

4. Wasserbauer, Joseph F.: Dynamic Responses of a Mach 2.5 Axisymmetric Inlet with Engine or Cold Pipe and Utilizing 60 Percent Supersonic Internal Area Contraction. NASA TN D-5338, 1969.

5. Cole, Gary L.; Neiner, George H.; and Crosby, Michael J.: An Automatic Restart Control System for an Axisymmetric Mixed-Compression Inlet. NASA TN D-5590, 1969.

6. Coltrin, Robert E.; and Choby, David A.: Steady-State Interactions from Mach 1.98 to 2.58 Between a Turbojet Engine and an Axisymmetric Inlet with 60-Percent Internal Area Contraction. NASA TM X-1780, 1969.

7. Calogeras, James E.: Experimental Investigation of Dynamic Distortion in a Mach 2.50 Inlet with 60 Percent Internal Contraction and its Effect on Turbojet Stall Margin. NASA TM X-1842, 1969.

8. Braithwaite, Willis M.; and Vollmar, William R.: Performance and Stall Limits of a YTF30-P-1 Turbofan Engine with Uniform Inlet Flow. NASA TM X-1803, 1969.

9. Mays, Ronald A.: Inlet Dynamics and Compressor Surge. Paper No. 69-484, AIAA, June, 1969.

10. Bellman, Donald R.; and Hughes, Donald L.: The Flight Investigation of Pressure Phenomena in the Air Intake of an F-111A Airplane. Paper No. 69-488, AIAA, June, 1969.

TABLE I. - VOLUMES OF J85-GE-13 ENGINE

Location	Axial length		Volume	
	ft	m	ft^3	m^3
Inlet subsonic diffuser (Mach 2.5 design)	3.42	0.1042	3.55	0.1005
Inlet subsonic diffuser (Mach 2.0)	3.94	.1201	4.04	.1144
Inlet guide vanes	.100	.0305	.1119	.00317
Stage 1	.1875	.0572	.1939	.00549
Stage 2	.1350	.0411	.1099	.00311
Stage 3	.1125	.0343	.0744	.00211
Stage 4	.0958	.0292	.0523	.00148
Stage 5	.0875	.0267	.0398	.00113
Stage 6	.0833	.0254	.0328	.00093
Stage 7	.0750	.0229	.0269	.00076
Stage 8	.0717	.0219	.0245	.00069
Outlet guide vanes	.0717	.0219	.0245	.00069
Compressor discharge plenum	.200	.0610	.187	.00530
Burner	.830	.2530	1.15	.03256
Turbine	.500	.1524	.158	.00447

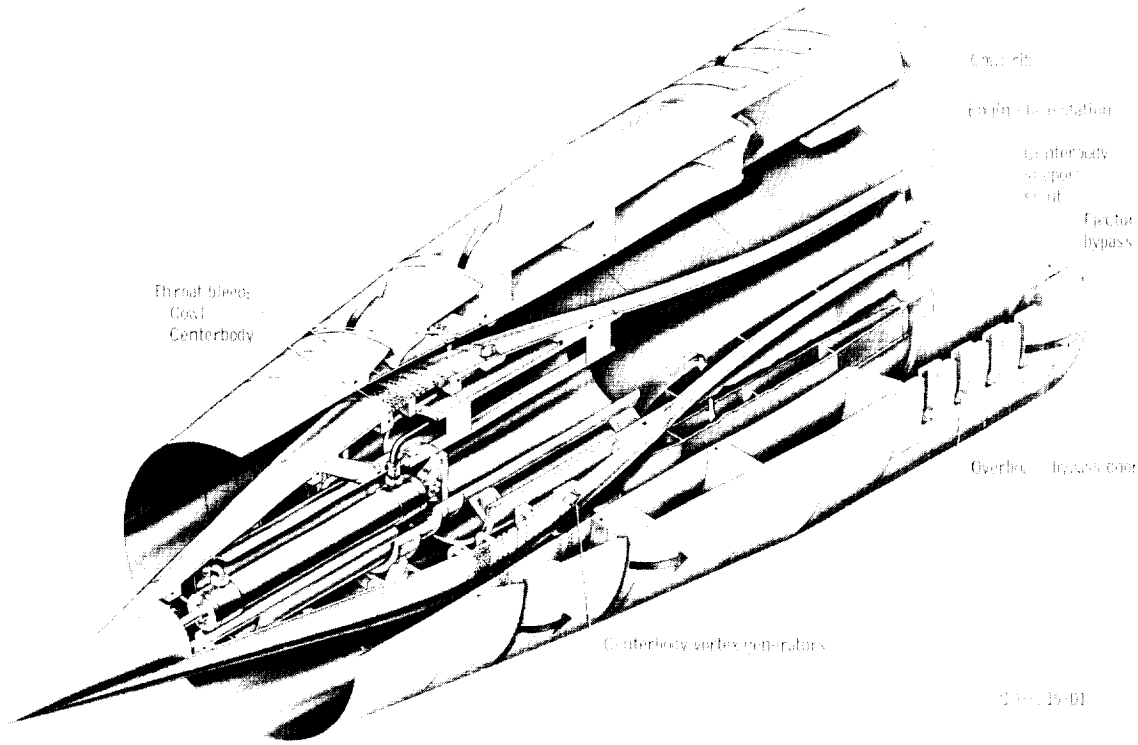

Figure 1. - Mixed compression inlet.

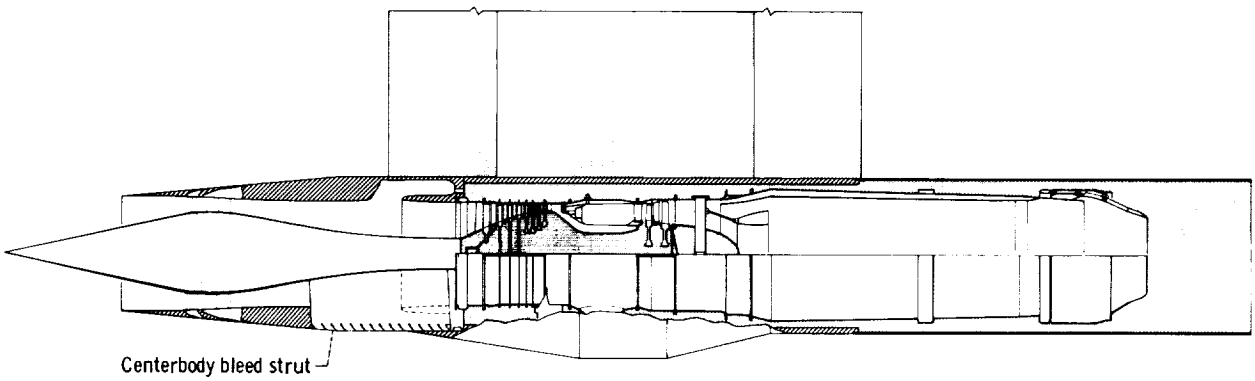

CD-9740-28

Figure 2. - Installation of J85-GE-13 turbojet engine.

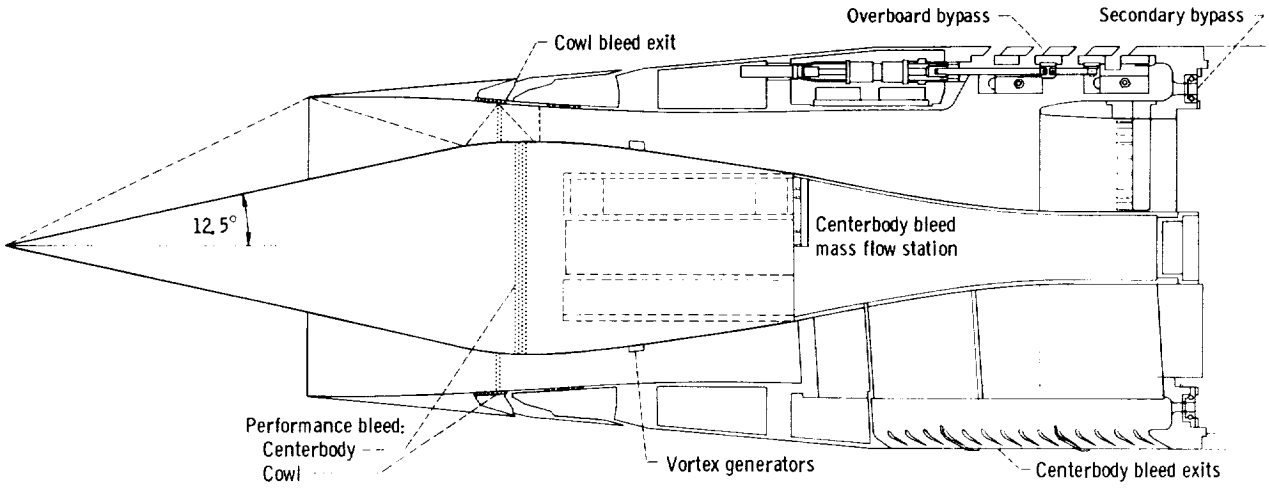

CD-9063-01

Figure 3. - Cross section of axisymmetric Mach 2.5 mixed compression inlet.

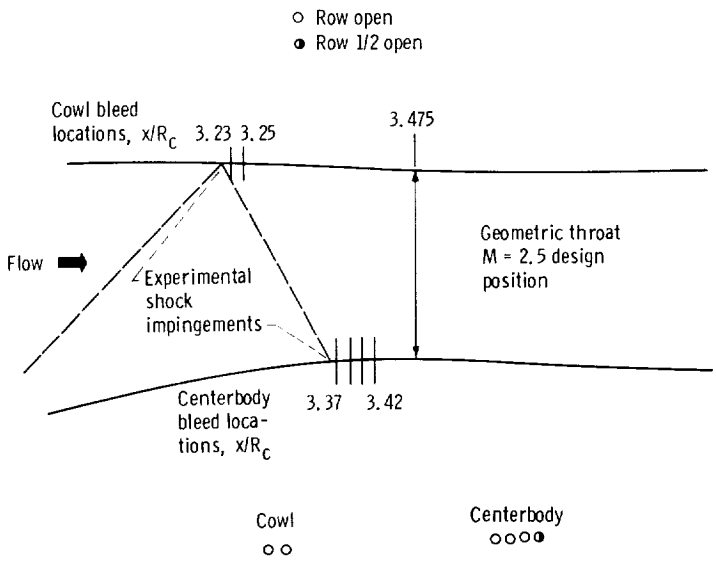

Figure 4. - Amount and location of performance bleed. All bleed holes 0.125 inch (0.379 cm) diameter.

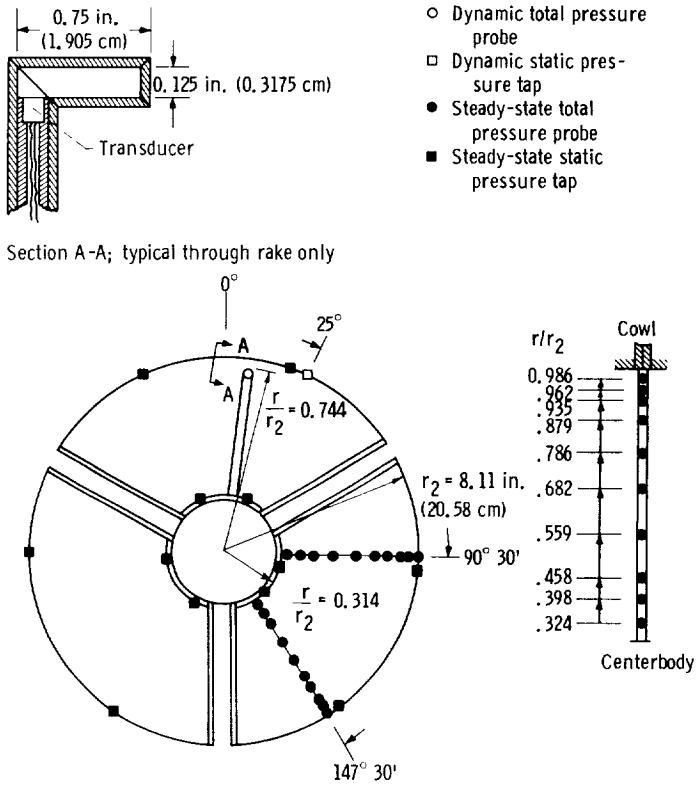

Figure 5. - Dynamic and steady-state compressor face (station 2) instrumentation. Downstream view.

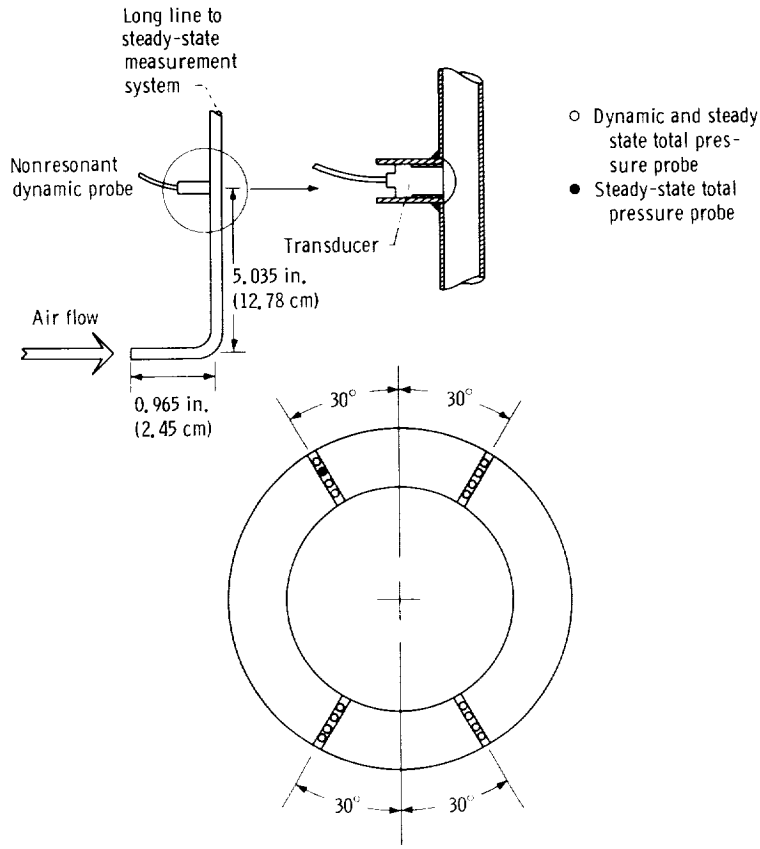

Figure 6. - Compressor discharge (station 3) instrumentation. Downstream view.

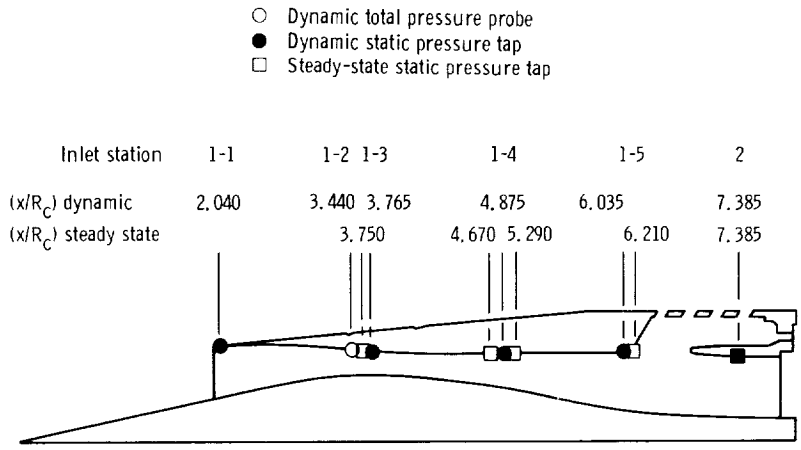

Figure 7. - Location of dynamic and steady-state pressure taps through inlet.

Location of dynamic taps

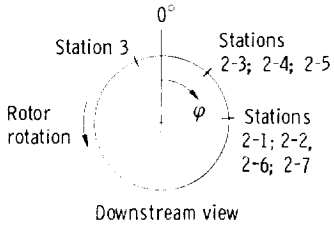

Station	Circumferential location, φ, deg			
	Dynamic taps		Steady-state taps	
	Static	Total	Static	Total
2-1	71.25	-----	22.5 and 337.5	---------
2-2	72.50	-----	22.5 and 337.5	---------
2-3	13.00	-----	22.5 and 337.5	---------
2-4	13.50	-----	22.5 and 337.5	---------
2-5	13.70	-----	22.5 and 337.5	---------
2-6	68.80	-----	22.5 and 337.5	---------
2-7	71.00	-----	22.5 and 337.5	---------
3		330.0		See fig. 6

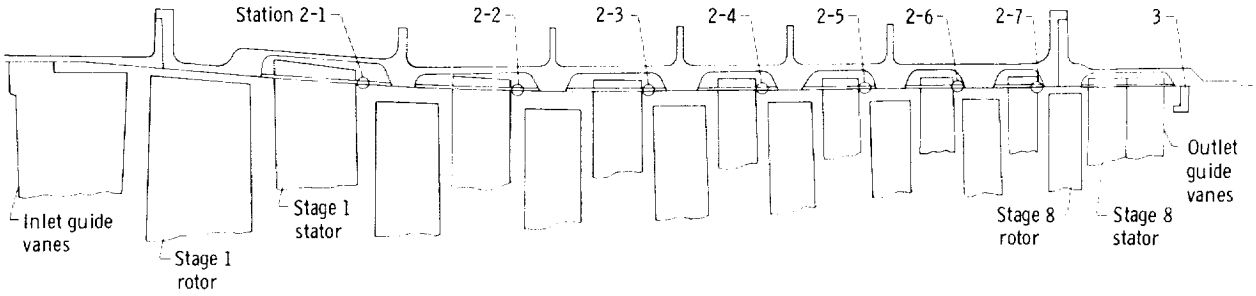

Figure 8. - Transient and steady-state instrumentation through compressor.

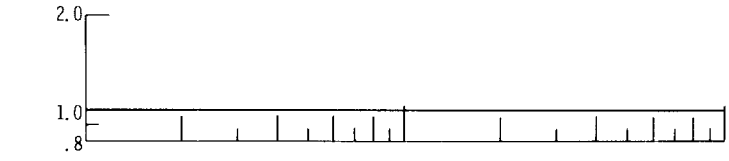

(a) Compressor face total pressure and inlet flush-mounted transducers.

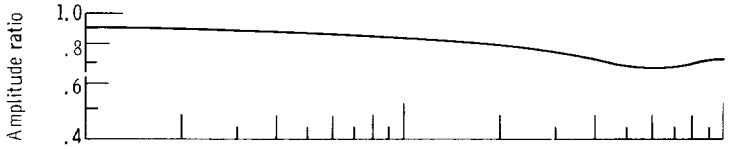

(b) Compressor exit total pressure.

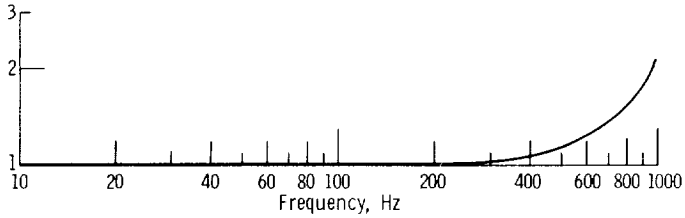

(c) Interstage compressor static pressure.

Figure 9. - Frequency response of transient pressure measuring systems.

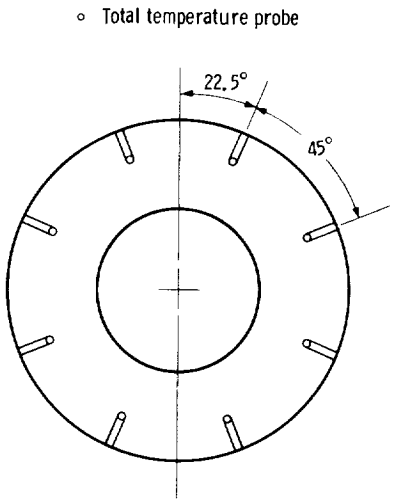

Figure 10. - Turbine discharge total temperature instrumentation. Downstream view.

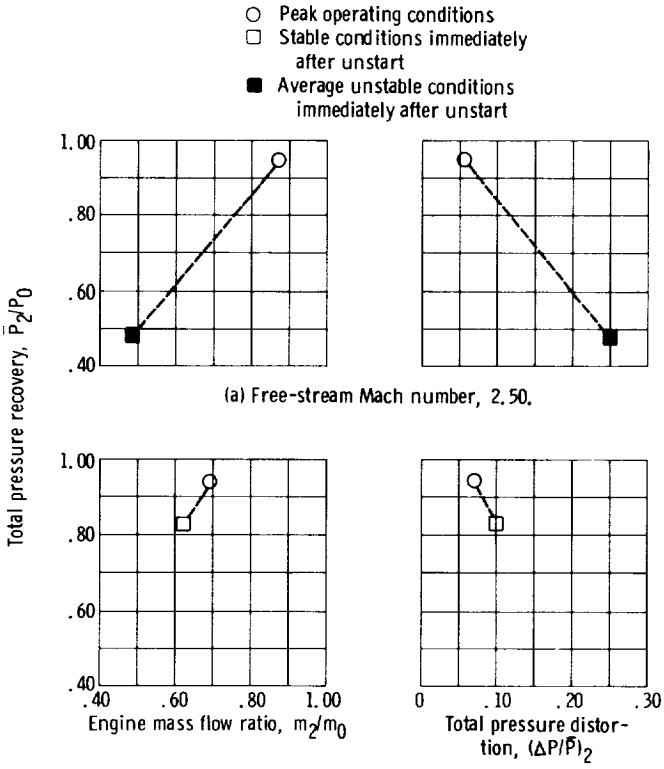

Figure 11. - Relative magnitudes of inlet unstarts at various free-stream Mach numbers.

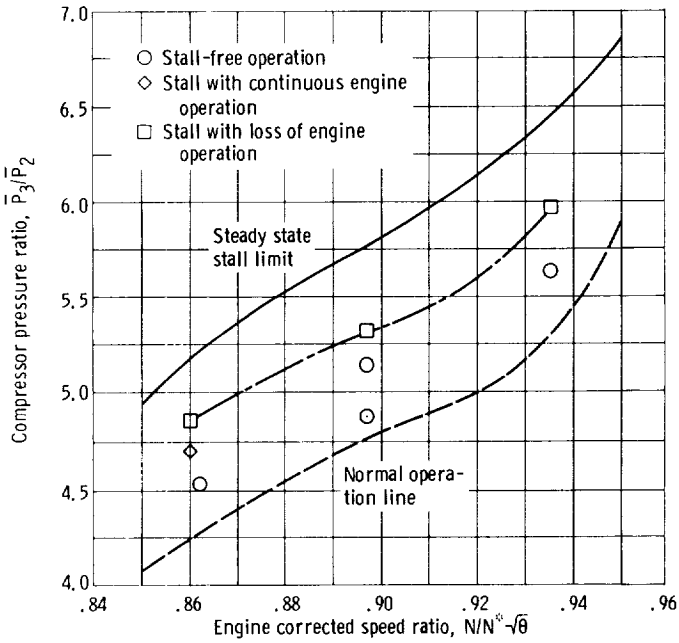

Figure 12. - Correlation of initial operating point to stall-free operation of J85-GE-13 engine during inlet unstart at Mach 1.98.

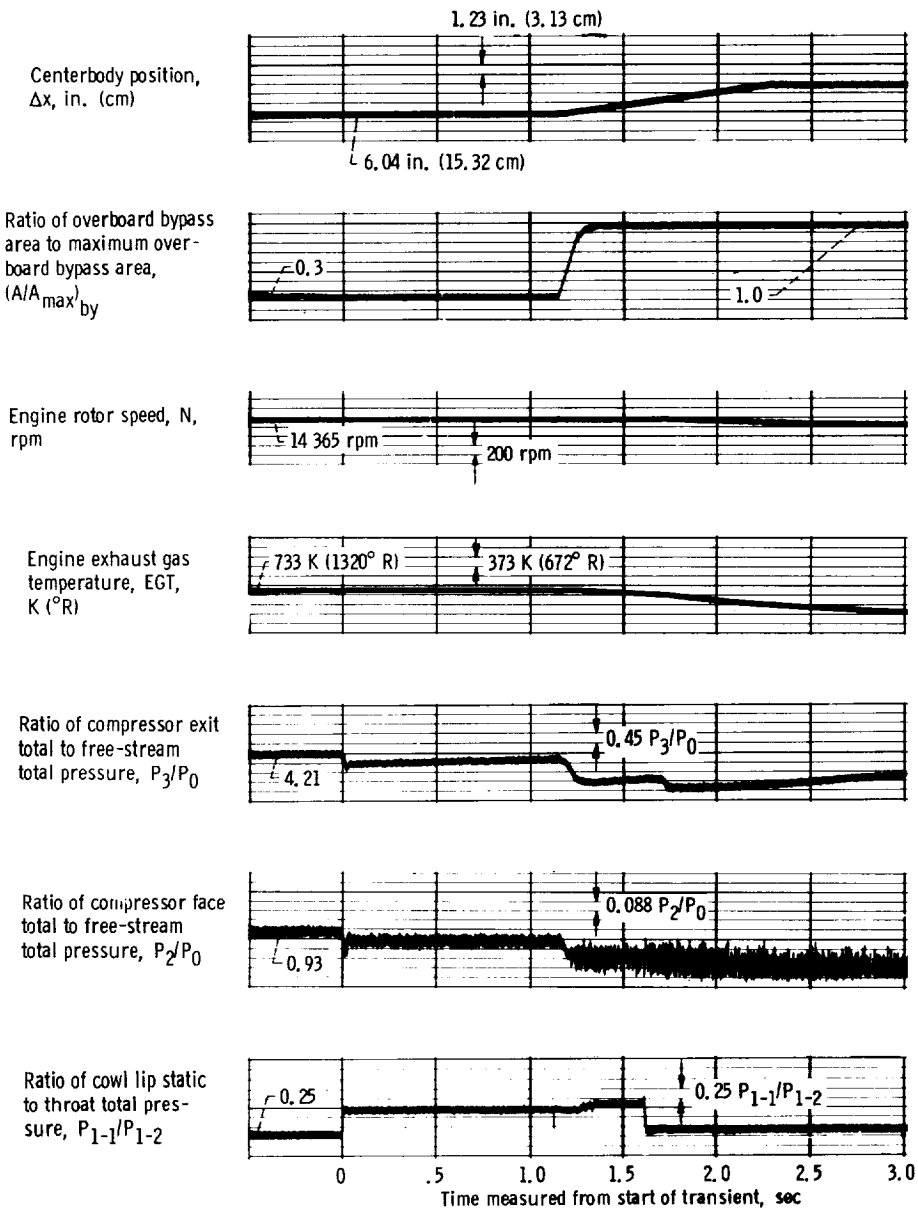

(a) Unstart with stall-free operation. Compressor pressure ratio, $\bar{P}_3/\bar{P}_2$, 4.56.

Figure 13. - Time history of inlet and engine parameters during an inlet unstart at Mach 1.98. (Positive displacements upward.)

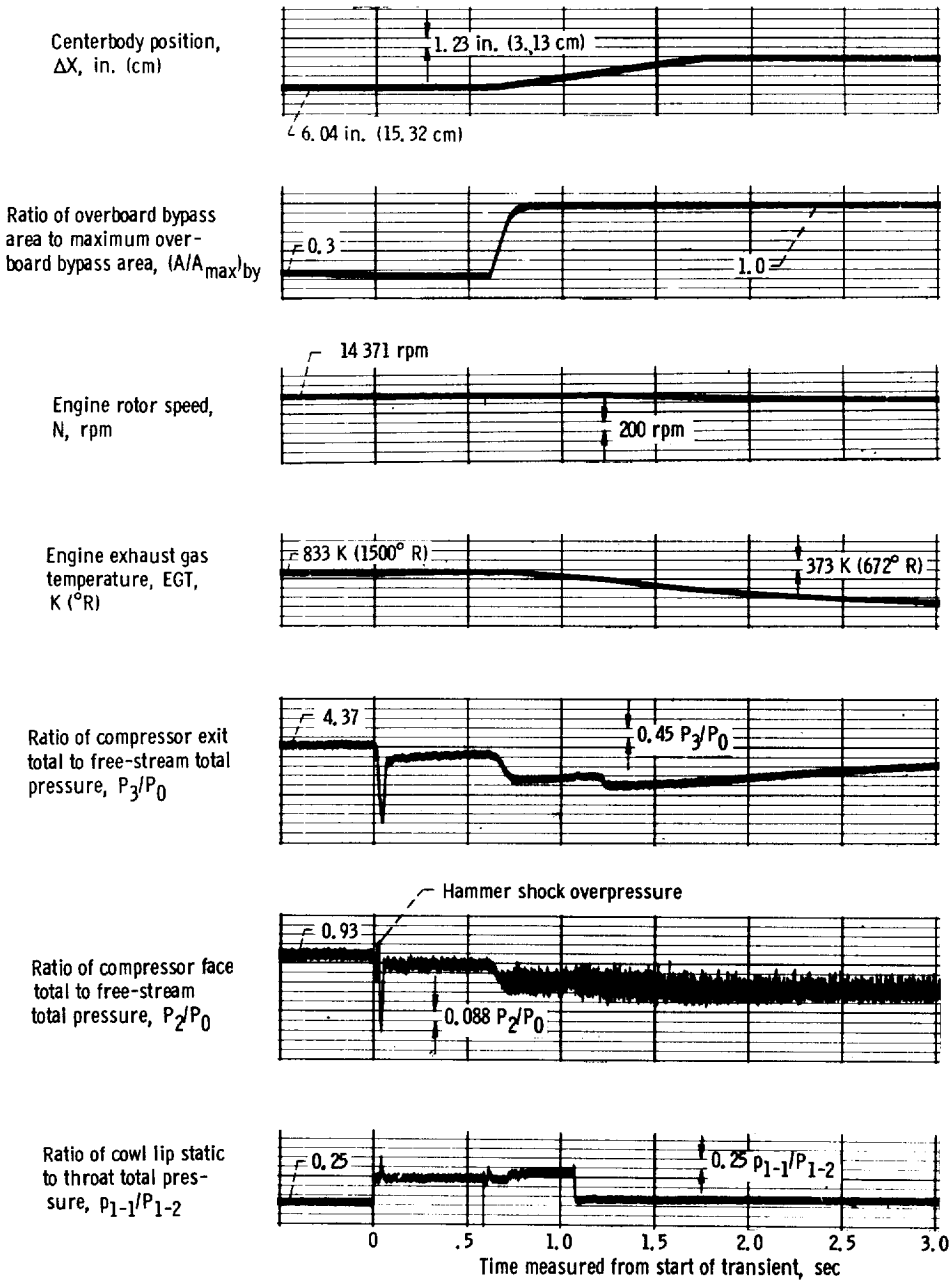

(b) Unstart with stall and continuous engine operation. Compressor pressure ratio, $\bar{P}_3/\bar{P}_2$, 4.69.

Figure 13. - Continued.

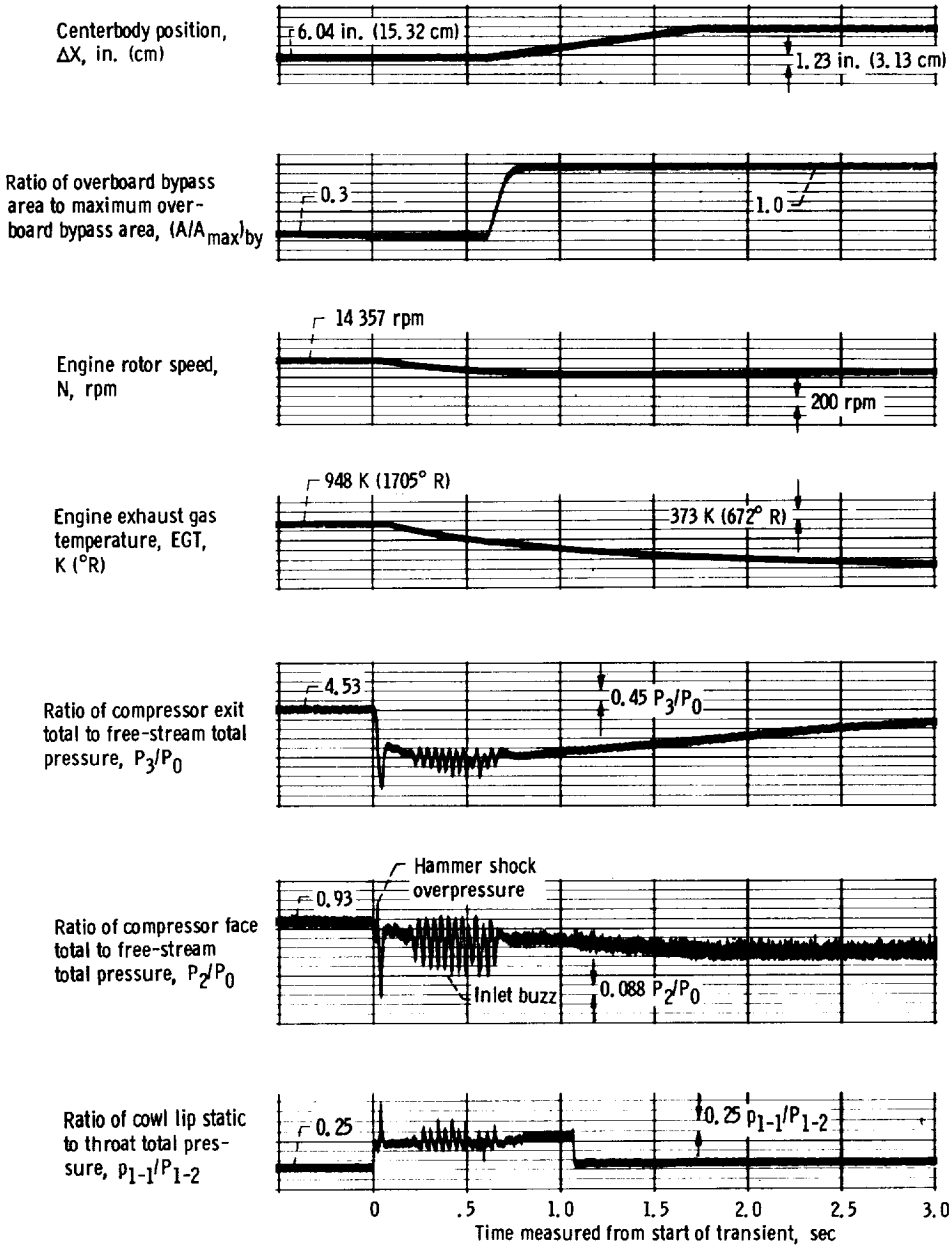

(c) Unstart with stall and loss of engine operation. Compressor pressure ratio, P_3/P_2, 4.87.

Figure 13. - Concluded.

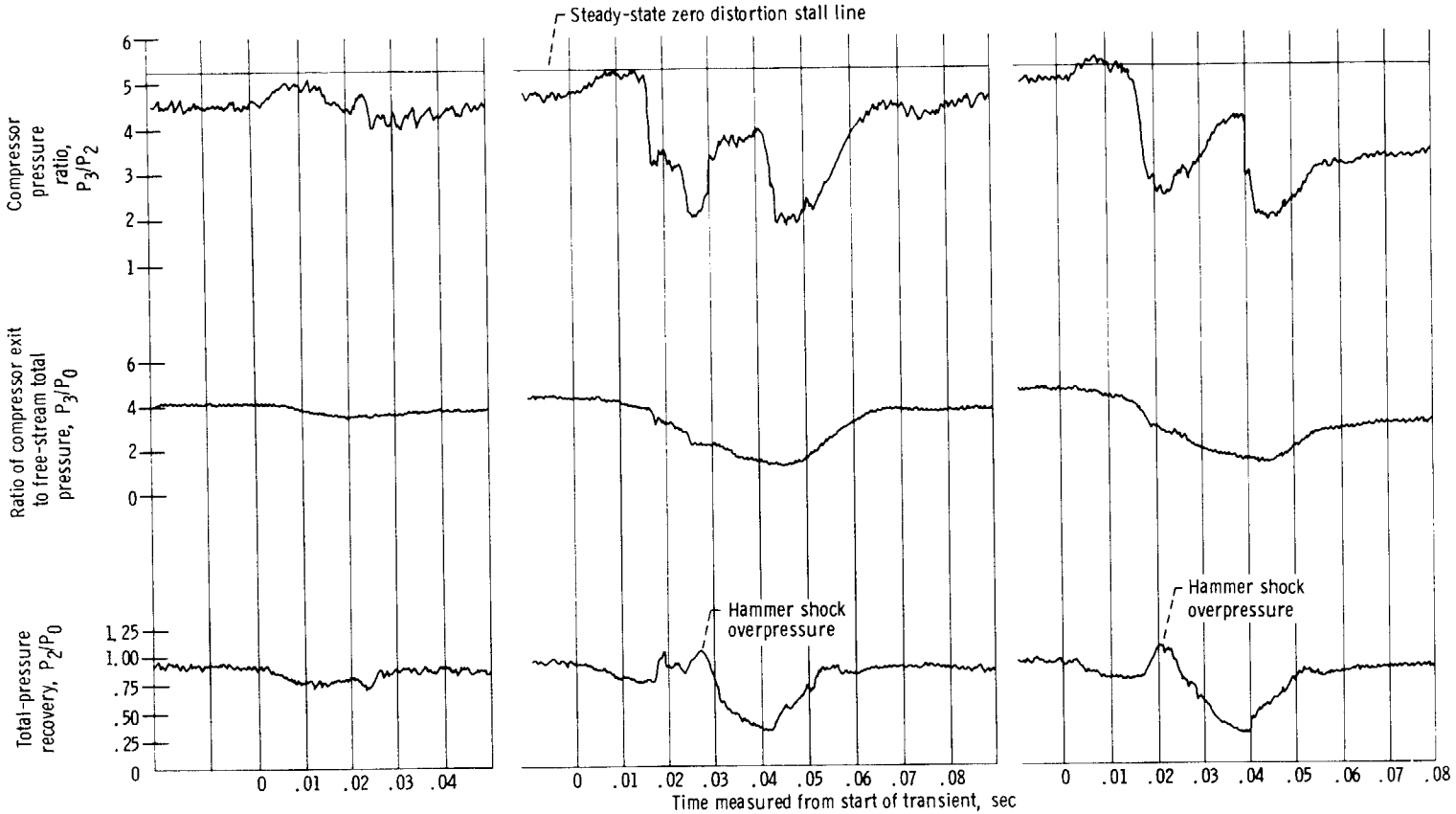

(a) Stall free operation. (b) Stall with continuous engine operation. (c) Stall with loss of turbine temperature.

Figure 14. - Correlation of dynamic compressor pressure ratio during inlet unstart to steady-state stall limit of J-85-13 at Mach 1.48. Corrected speed ratio, $N/N^* \sqrt{\theta} = 0.86$.

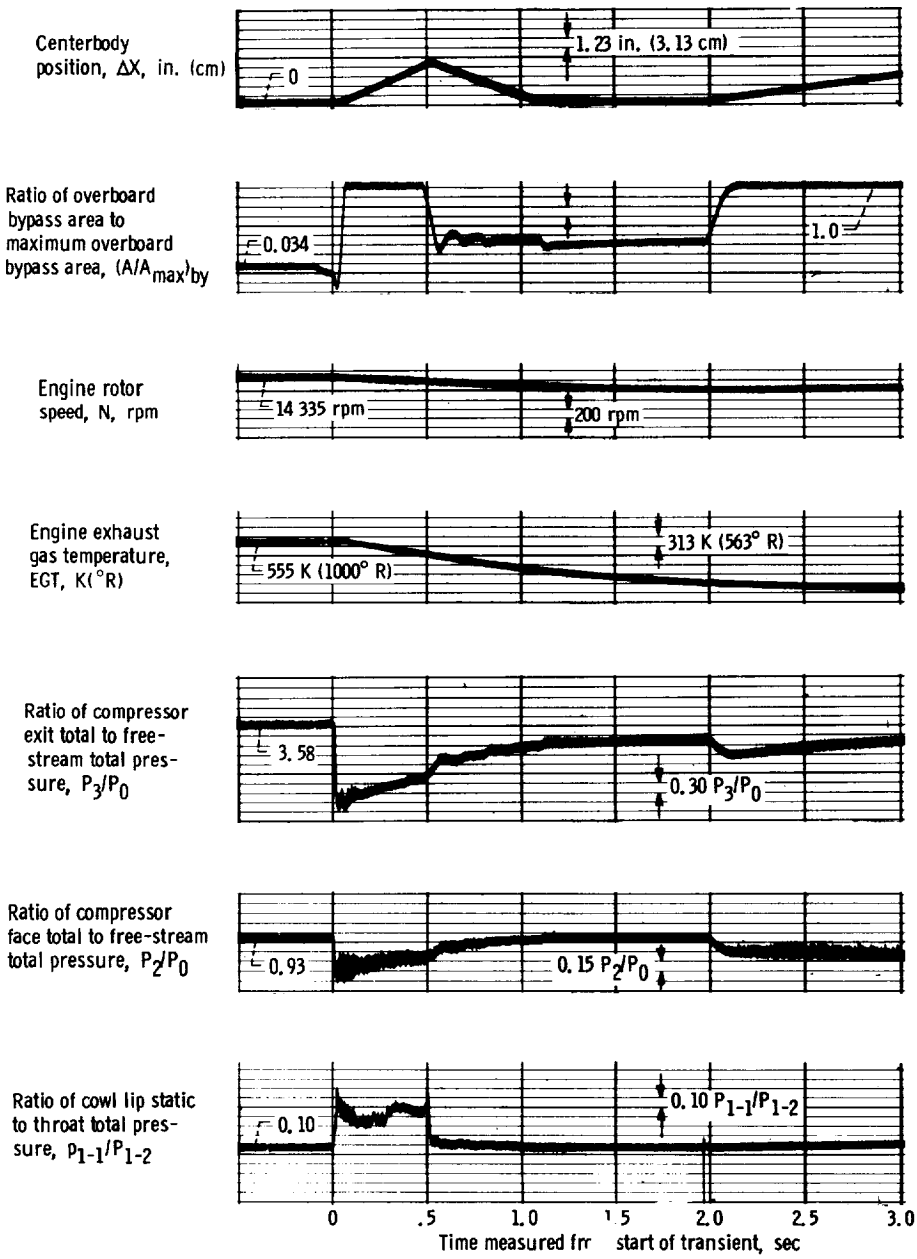

Figure 15. - Time history of inlet and er ıe parameters during inlet unstart at Mach 2.5. Engine corrected speer /N* -√θ, 0.85.

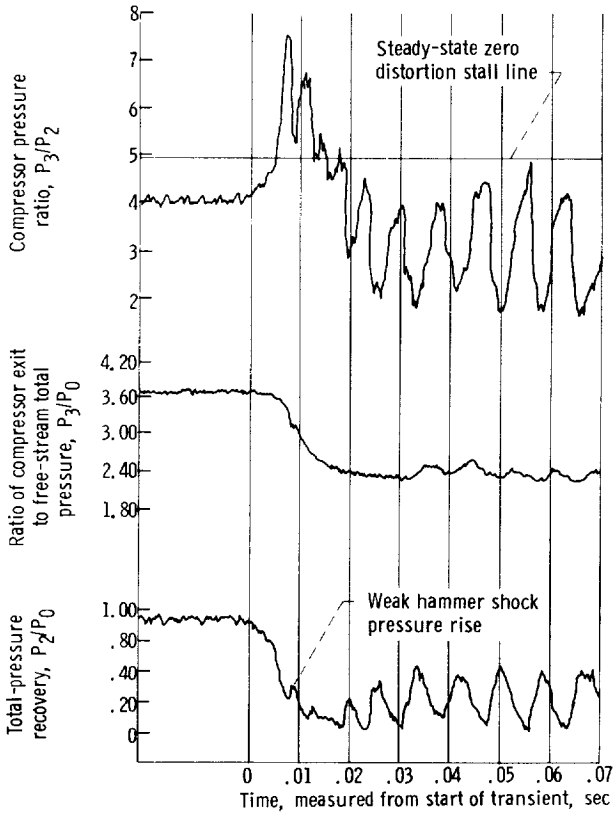

Figure 16. - Effect of inlet unstart on dynamic compressor pressure ratio at Mach 2.5. Corrected speed ratio, $N/N^* \sqrt{\theta} = 0.85$.

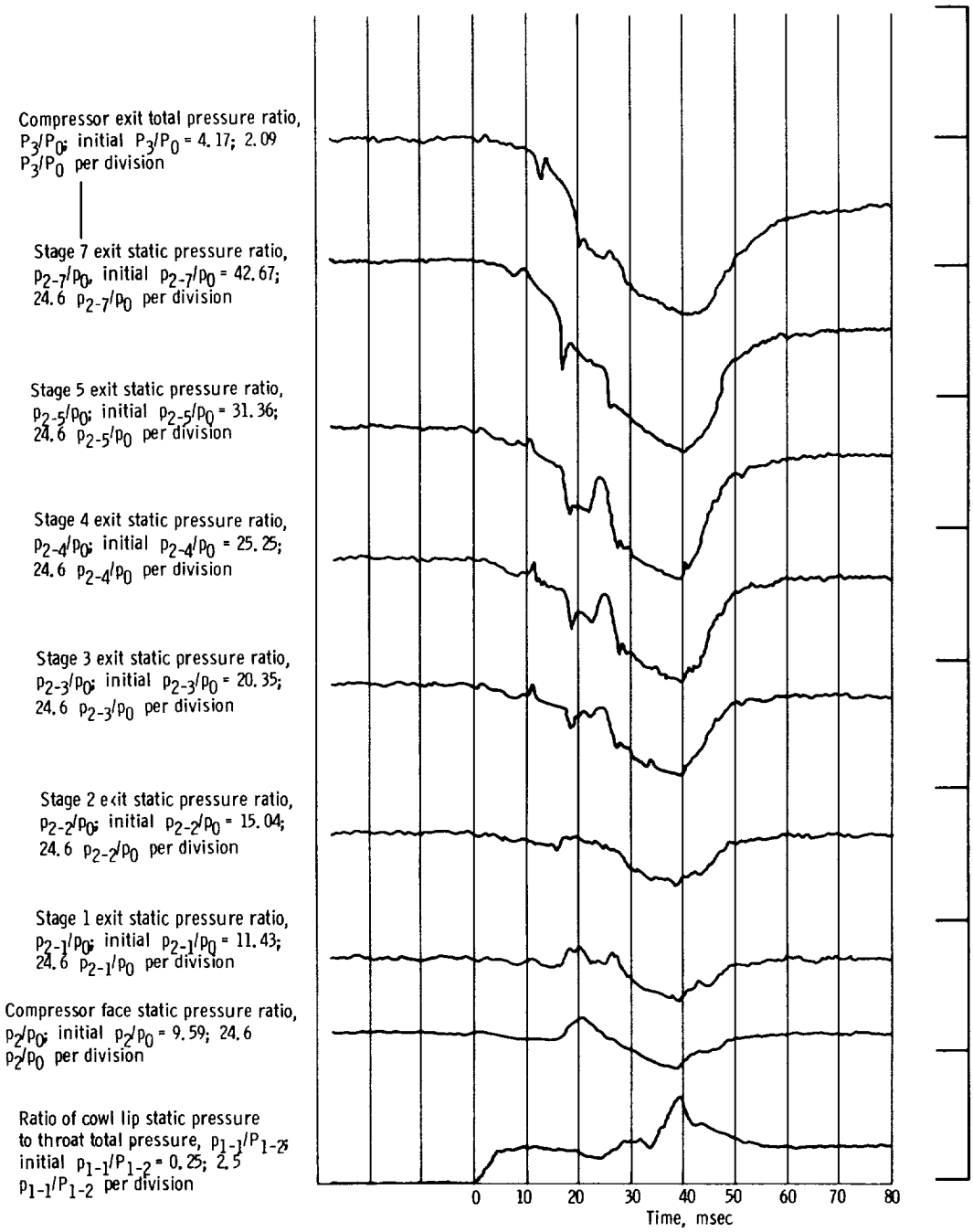

(a) Stall caused by inlet unstart. M_0 = 1.98, $N/N^\circ\sqrt{\theta}$ = 0.86, steady-state $\bar{P}_3/\bar{P}_2$ = 4.86.

Figure 17. - Time history of compressor pressures during compressor stall.

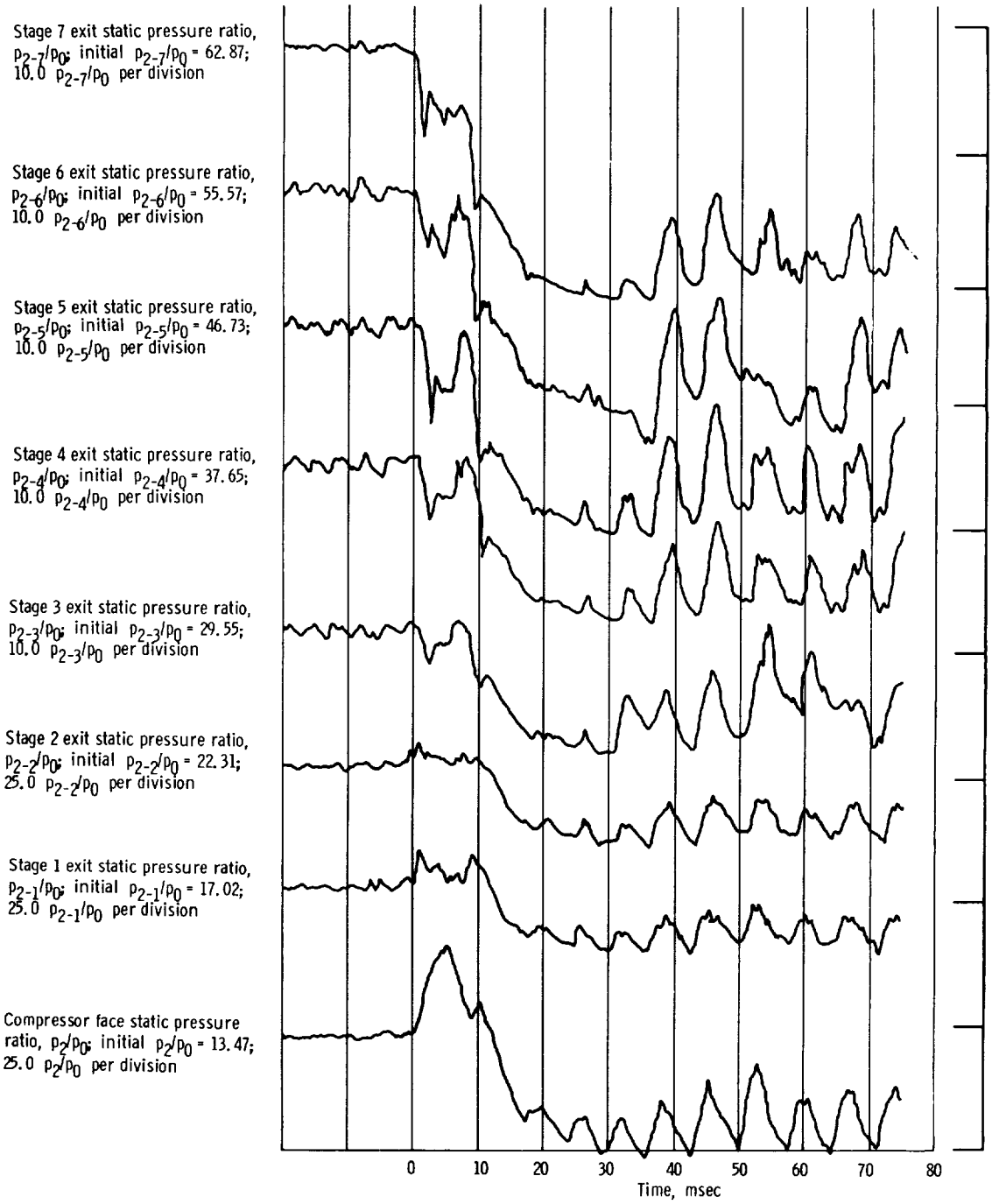

(b) Stall caused by decreasing primary nozzle exit area: $M_0 = 2.5$, $N/N^* \sqrt{\theta} = 0.88$, steady state $\bar{P}_3/\bar{P}_2 = 4.61$.

Figure 17. - Continued.

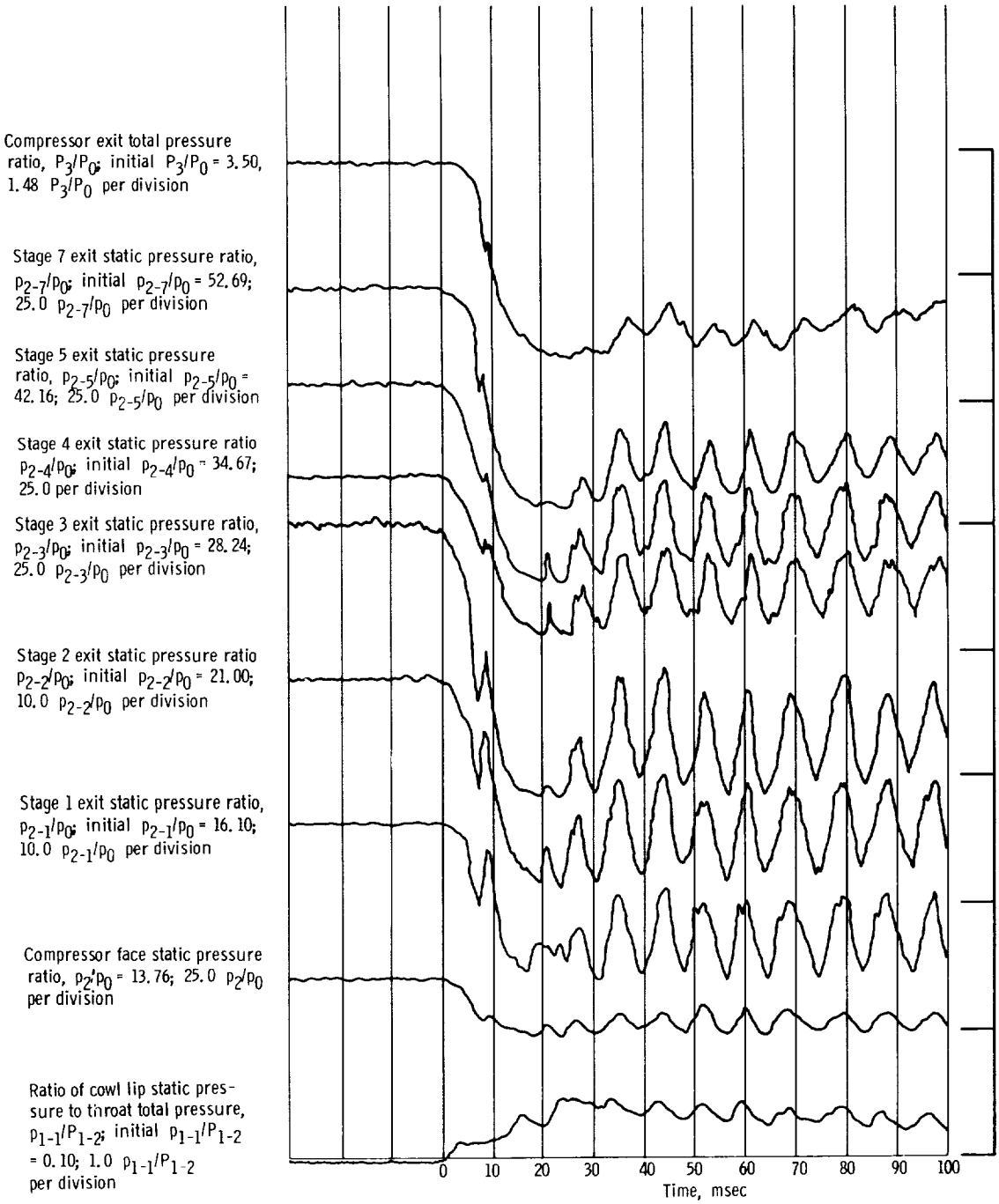

(c) Stall caused by inlet unstart. M_0 = 2.5, $N/N^\circ\sqrt{\theta}$ = 0.85, steady-state $\bar{P}_3/\bar{P}_2$ = 4.03.

Figure 17. - Concluded.

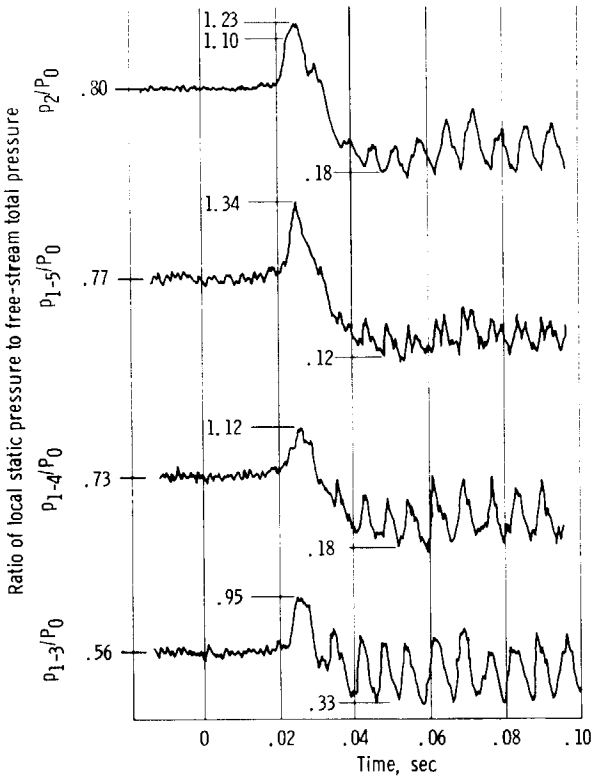

Figure 18. - Time history of inlet pressures after compressor stall at Mach 2.50.

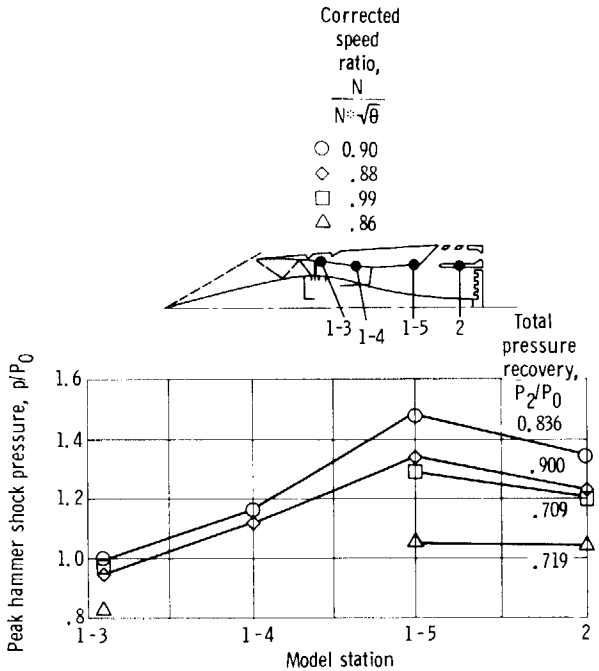

Figure 19. - Peak hammer shock pressures through inlet after compressor stall at Mach 2.5.

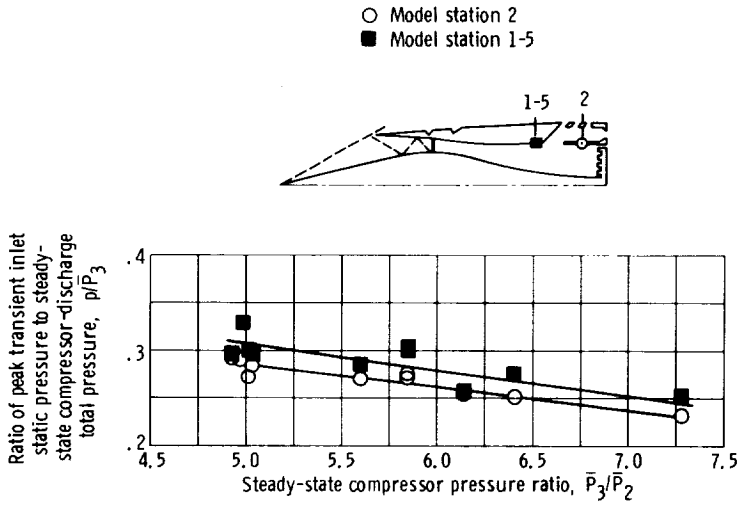

Figure 20. - Peak hammer shock static pressure as a function of compressor pressure ratio.

NASA-Langley, 1971 —— 28 E-5923